

Gear Geometry as a Function of the Production Method

Proposal of Invo-Planar bevel gears for good productivity with 5X-machine

A. Kubo and A. Ueda

Abstract In the frame of the activity of the JSME RC-268 committee, a new bevel gear, i.e., the Invo-Planar bevel gear, is developed, the tooth flank of the wheel of which is a plane or whose transverse tooth profile is a straight line. The cutting/grinding time for this bevel wheel can be more than 10 times shorter than the working time for a conventional bevel gear wheel, when it is cut with a 5-axis machining center, because it cuts or grinds the tooth flank through one path of tool movement. The finished tooth flank is far smoother than the curved tooth flank manufactured through many paths of the cutting blades of the tool. The production rate of the mating pinion with a 5-axis machining center is the same as that of a conventional bevel pinion. Some experiences in the production and quality assessment of product gears, and a performance survey of this new bevel gear, are introduced to promote discussion.

Keywords Bevel gear · Face gear · Design · Manufacturing · Induced stress · Surface integrity

1 Introduction

When we look at the history of gearing, we see that it began with pin or lantern gears. Initially, in cylindrical gears, the theory of the conjugate action of gear meshing was investigated and it was found that a good transverse tooth form was the main point of interest. Subsequently, the cycloid tooth form took up the primary position in the practical field of usage, but now, the involute profile prevails. The main factor driving this change is the fact that the involute gear system has

A. Kubo (✉)

Research Institute for Applied Sciences, Kyoto 606-8202, Japan
e-mail: aizokubo@hera.eonet.ne.jp

A. Ueda

AMTEC Inc., Prio Tower 4305, Osaka 552-0007, Japan
e-mail: ueda@amtecinc.co.jp

(1) a high efficiency production system using a basic rack form, (2) tools for high accuracy quality inspection and (3) the permissible strength and toughness of the product gears in practical usage.

There is now a major trend towards a change in the production method of big gears, especially big bevel gears: Until recently, all gears were produced with a specialized gear cutting and/or grinding machine, but now, a multipurpose 5-axis machine is often used for the production of big bevel gears with a sufficient accuracy grade. When we consider the history of gear technology as mentioned above, the production method decides the kind of gear that prevails in the field of practical usage. We can see this history in cylindrical involute gears, in worm gears, and in bevel gears. In addition, the gear production system using a 5-axis machine can be more flexible than the system consisting of specialized gear production machines alone. As a result, this trend of utilizing 5-axis machines for gear production will continue to prevail in the near future. The detail of the 3D dimension of the traditional bevel gear is the result of the Gleason and Klingelnberg machines and their production systems. Thus, the following question arises here: “Is today’s bevel gear optimal for production with a 5-axis machine?” This report details a trial designed to find the optimal bevel gear for 5-axis machine production.

One of the problems of gear production with a 5-axis machine is the efficiency of gear tooth cutting or grinding, i.e., the time needed to produce the curved and twisted 3D surface of tooth flanks is too long. For gear manufacturing, many paths of the movement of a cutting/grinding tool are necessary to realize the conjugate 3D curved surface of the tooth flanks, and long manufacturing time means greater production cost. Another problem is the surface integrity of tooth flanks finished with a 5-axis machine: the surface roughness is especially insufficiently smooth in comparison with a tooth flank finished with conventional specialized gear production machinery. The task we have to solve is how such demerits of gear production with a 5-axis machine can be improved so as to draw out the merits of this new production method for realizing better big gears.

2 Way of Thinking

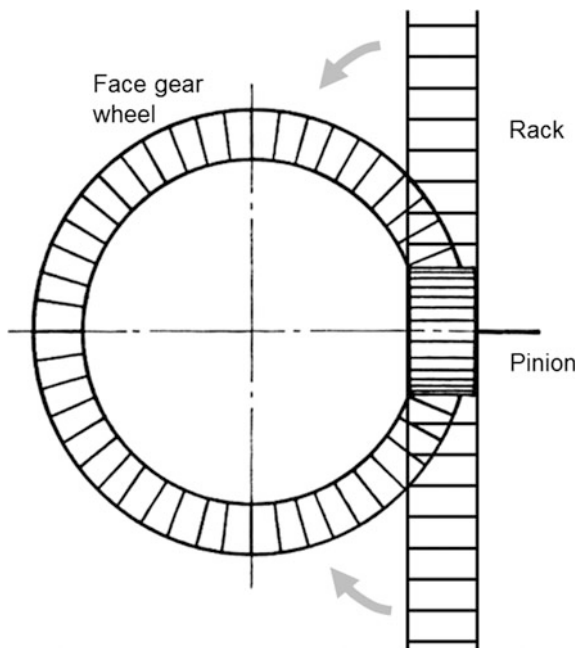
First, we consider an involute rack and pinion in mesh. Then, we bend the rack in the horizontal plane to make a circle, as shown in Fig. 1. Such a system consisting of a pinion and a horizontal circular wheel is known as a Face Gearing system. The mechanical action of the bevel gears can be replaced with face gears. This is the reason why we take face gears as the starting point for developing new bevel gears that can be better produced with a 5-axis machine. The pinion of face gearing is, e.g., of a cylindrical involute gear, and there is no difficulty in producing it. The wheel, however, is a tough problem: The pressure angle at the heel becomes small and the greater part of the dedendum is covered with an unworkable, big tooth fillet curved surface. The pressure angle at the toe becomes very large, making tooth crest into a sharp point (see Fig. 2). When we want to take a reasonable amount of

the tooth width for gear performance, or when we want to take the small tooth number of a wheel to create a somewhat smaller gear ratio, the wheel tooth can no longer exist in a reasonable form.

For this reason, it is not easy to design face gears whose ratio is less than ca. 4. This brings up a common difficulty in designing a power transmission gear box with face gears. In addition, the transverse tooth form of the wheel is almost a straight line, like the rack tooth form, but it is slightly convex, and by an amount that is not negligible. This condition brings up a big problem in producing the face gear wheel economically. These are the reasons why we cannot utilize face gears well in practical fields of usage.

The solution to this problem, however, is not difficult: When we use a conical involute pinion that has somewhat of the same cone angle as that of normal bevel gears (see Fig. 3), the pressure angle at the toe and the heel approaches a reasonable value. The tooth profile of the wheel is almost a straight line, but it is still a little bit convex, because the teeth number is not infinity. When we replace this curved transverse tooth form of the wheel with a straight line and give the corresponding amount of 3D tooth form modification to the tooth flank form of the mating pinion, we have a gear set that does not lose the conjugate action of gear meshing. We call this gear set “Invo-Planar bevel gears of the 2nd kind.” The amount of 3D form modification of the pinion tooth flank from the tooth flank of the involute conical gear is not significant. It can then be ground with a grinding machine for cylindrical involute gears, when adequate software for NC control and a corresponding grinding tool is developed.

Fig. 1 Transformation of rack and pinion to a face gear set



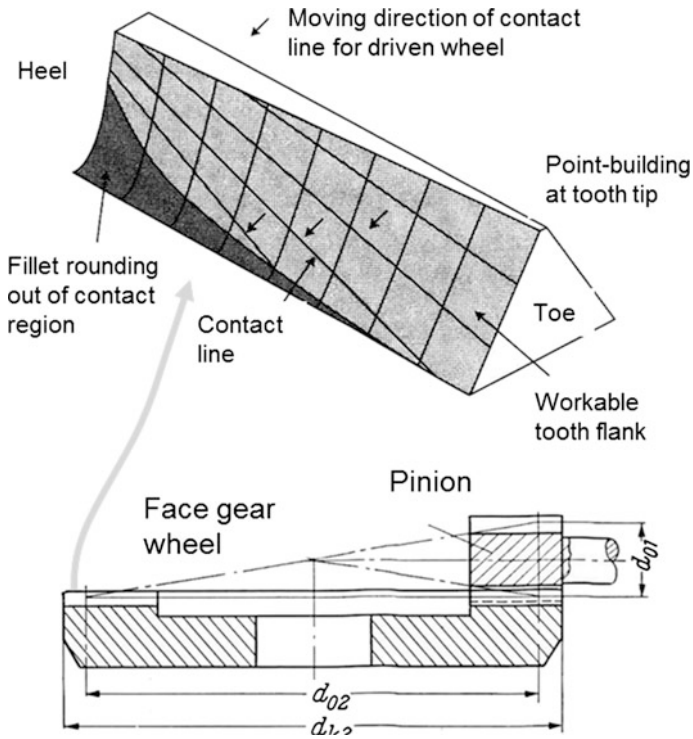


Fig. 2 Face gear set and tooth form of the wheel

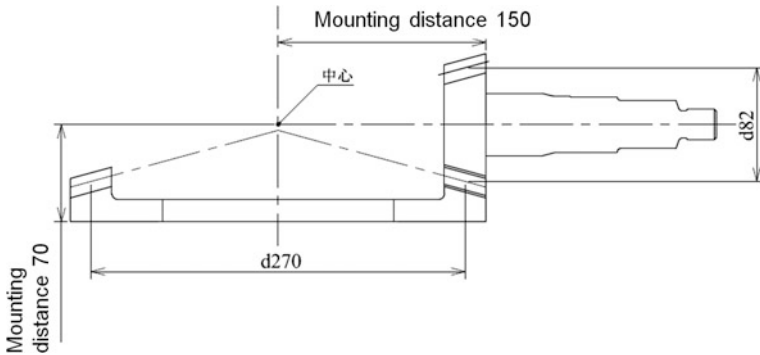


Fig. 3 Conical pinion and mating face gear wheel

The small difference in the pressure angle at the toe and the heel of this bevel wheel then suggests an idea: that we can replace the whole tooth flank of the wheel with a pure plane. Of course, the 3D tooth flank form correction of the mating tooth flank of the pinion must be changed to realize the conjugate action. We call this

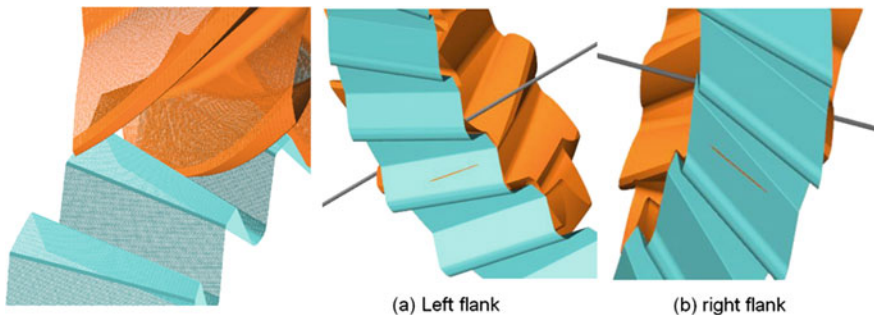


Fig. 4 Tooth meshing of IPB gears and the contact line

gear set with a very simple plane tooth flank form “Invo-Planar bevel gears of the 1st kind,” referring to “IP-bevel gears” or “IPB gears.” The tooth flank of the IPB wheel can be manufactured by one path of the cutting/grinding tool. The production rate of the wheel is then drastically accelerated by reducing and minimizing the number of cutting/grinding tool paths for forming the tooth flank. The production rate of the IPB pinion with a 5-axis machine, however, remains the same as the working time for conventional bevel pinion production.

3 Invo-Planar Bevel Gear

The leftmost picture in Fig. 4 shows how the IPB gears mesh to transmit motion and power. The center and rightmost figures in Fig. 4 show the contact line on the plane tooth flank of the wheel.¹ The simulation was carried out to visualize the contact line by bringing a very small amount of interpenetration of the pinion tooth flank into the wheel tooth flank by using a CAD model. The figure sees this state from inside the wheel. It is well-recognized that line contact is realized: this is quite a natural matter, of course, because the IPB gear is a strong modification of the involute rack and pinion, as explained above.

The two uppermost pictures in Fig. 5 are the tooth contact pattern obtained by moving the contact line shown in Fig. 4 under the constant rotational speed of both the pinion and the wheel. You can see that the amount of interpenetration between the tooth flanks of the pinion and the mating wheel stays constant during gear rotation. This comes from the fact that this motion is a conjugate action of the rotational angle transmission of the IPB gearing. The lowermost two pictures in Fig. 5 show the distribution of relative slipping velocity between the mating tooth flanks of the pinion and the wheel. The constant slip-velocity line on the pinion

¹In this CAD model, the tooth flank form of the IPB wheel at the tooth edges is gradually and smoothly modified from the plane, so as not to cause edge contact at the gear mesh.

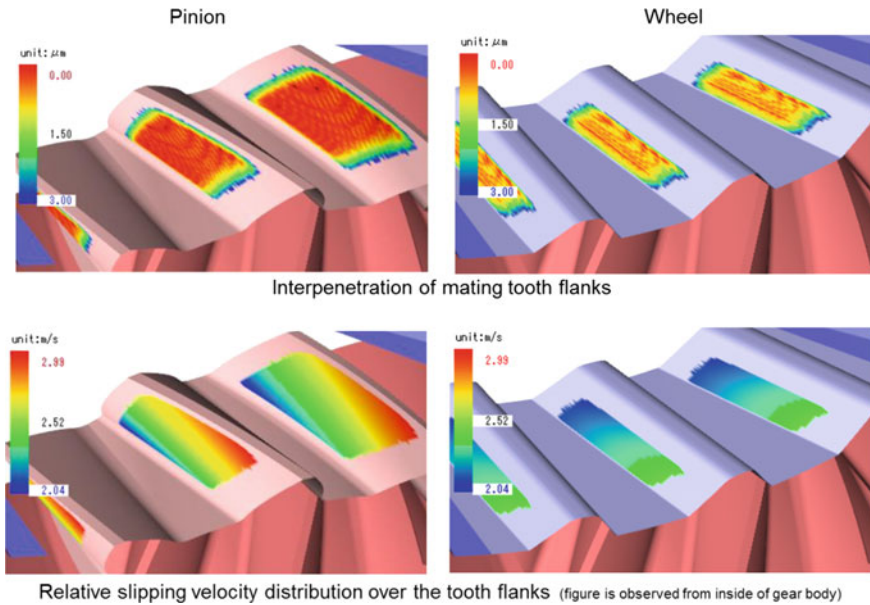


Fig. 5 State of tooth flank contact and slipping velocity distribution

tooth flank is somewhat inclined in the same manner as a common face gear meshing. In this gear design, the pitch line (the rolling contact line) looks to be lower than the dedendum of the pinion tooth flank. The slipping velocity on the wheel tooth flank is changing longitudinally in the tooth width direction. The slipping velocity increases in the direction of the near heel, but the difference is not much at the toe and heel.

4 Production

For this investigation, gear material JIS SCM420H is taken, and both the wheel and pinion are roughly cut with a flat end mill, as shown on the left sides of Figs. 6 and 10. Then, they are case carburized and hardened, and their tooth flanks are finished with a CBN electro-deposited disk grinding tool. The operation is shown on the right sides of Figs. 6 and 10. The final finishing touch of the wheel tooth flank is worked out by one path of tool movement in the lead direction, with a grinding speed of 2034 m/min, a feed of 0.012 mm/rev, and a grinding depth of 5 μm . The pinion tooth flank is ground by many paths of tool movement in the lead direction, with step 0.4 mm in the tooth form direction, a grinding speed of 2034 m/min, a feed of 0.012 mm/rev, and a grinding depth of 5 μm .

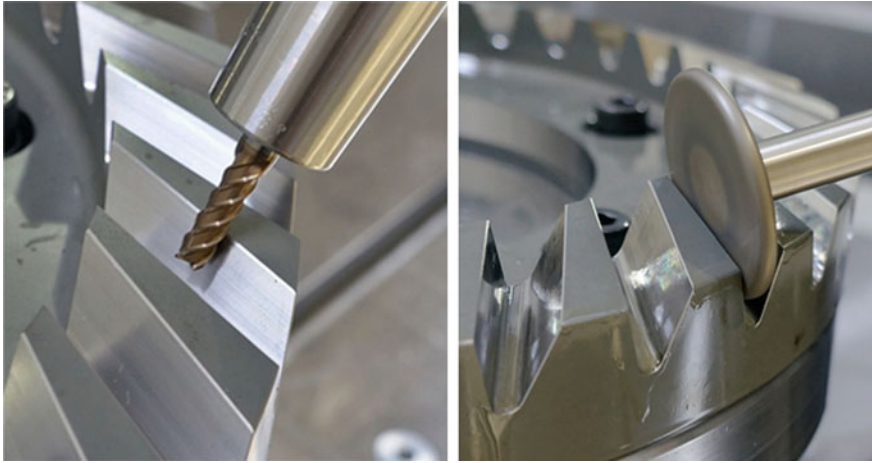


Fig. 6 Rough-cutting and finish-grinding of IPB wheel teeth

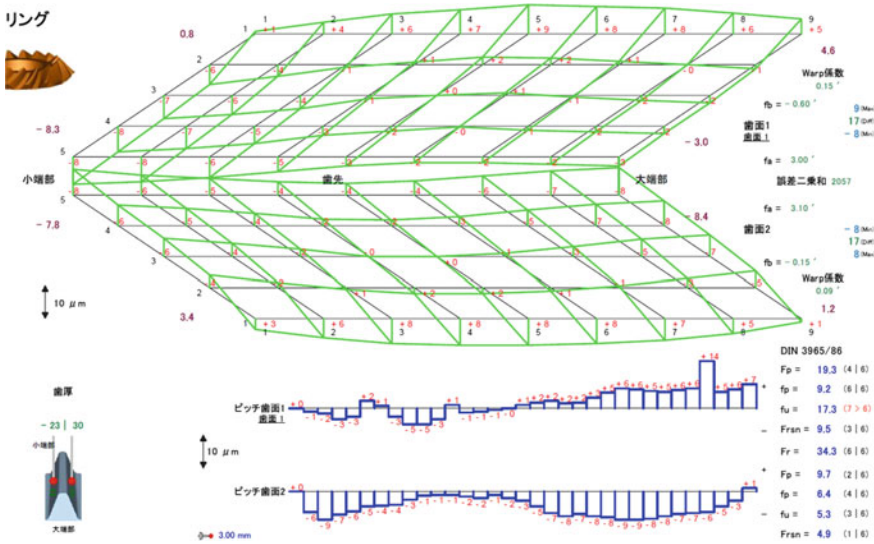


Fig. 7 Pitch and tooth flank form accuracy of an IPB wheel

The completed gears are examined in the 3D form accuracy of the tooth flank. Figure 7 shows the results measured with a high precision CMM. The definition of the form accuracy is the form deviation between the actual tooth flank and the CAD data of the IPB wheel. The gear accuracy is better than ca. 7 μ m. Figure 8 is the detailed 3D form deviation of one whole tooth flank measured with a high

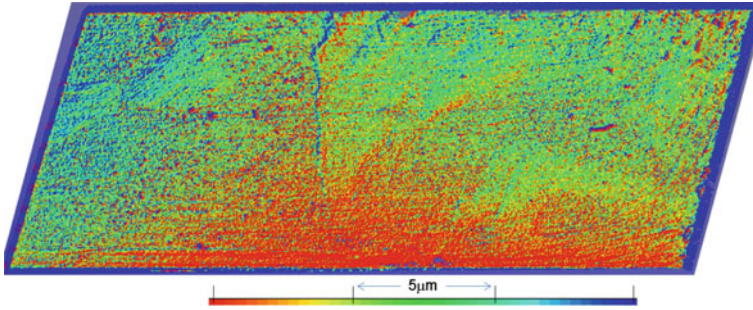


Fig. 8 3D form accuracy of a whole tooth flank

precision, contact-free 3D form-checker using the light beam cutting method. The peak to valley amplitude of the grinding mark on the tooth flank is ca. $0.3\text{--}0.4\ \mu\text{m}$, but they are well-measured. Figure 9 shows the form accuracy of the whole wheel teeth measured with the same contact-free form inspection machine. The geometrical form of all tooth flanks is well-manufactured (Fig. 10).

Figure 11 shows the measured tooth flank form deviation of the pinion. The form deviation of the pinion tooth flank is about 2 times worse than that of the wheel. This result, perhaps, from (1) the polygon effect of the grinding paths needed to form the 3D tooth flank and (2) the difficulty of simultaneous 5-axes NC control during the grinding operation in comparison with the grinding of a plane.

5 Estimated Performance

The induced tooth fillet stress is examined by using FEM analysis. The same analysis was carried out with a spherical involute bevel gear of the same size. The tooth root and fillet form of the spherical involute bevel gear is optimized to minimize the induced stress. Much of our analysis shows that the induced fillet stress of such a spherical involute bevel gear is somewhat lower than that of conventional bevel gears after a normal Gleason or Klingelberg system. This is the reason why we take spherical involute bevel gears as the object for comparison in induced tooth root stress to evaluate the IPB gears.

Figures 12 and 14 show the form of gear teeth of these two kinds of bevel gear, incorporated for comparison. The load is applied to the FEM nodes at the tooth tip, in the normal direction of the tooth flank, and the total amount of loading is 10 kN. Figures 13 and 15 show the state of induced tooth fillet stress and their maximum value. The induced stress of the IPB wheel is somewhat smaller than that of the spherical involute bevel wheel. When we see Fig. 12, we note that the tooth thickness of the IPB wheel looks too large: this is because the design for sharing tooth thickness between wheel and pinion is still not well done; that is the task of development to come. This means that the width of this wheel tooth should be

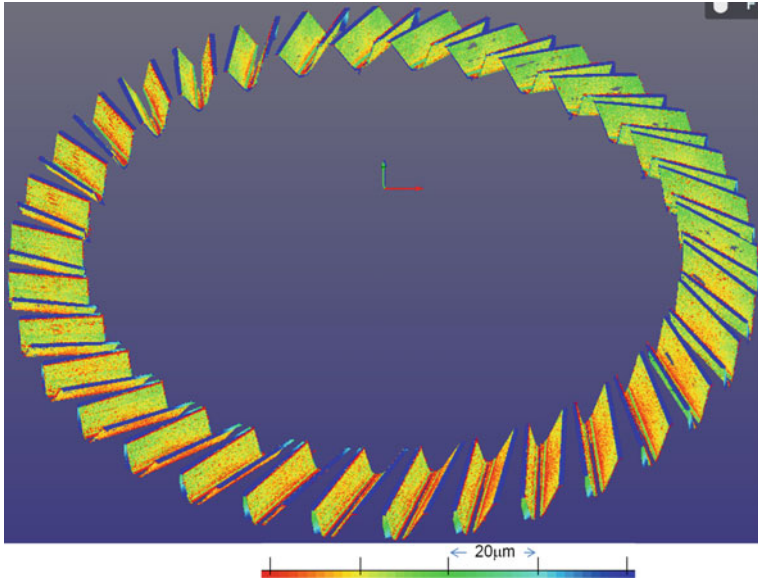


Fig. 9 Accuracy of all the teeth of an IPB wheel



Fig. 10 Rough-cutting and finish-grinding of IPB pinion teeth

reduced to some extent, and the pinion tooth thickness should correspondingly increase. It is really remarkable that the induced stress of the IPB pinion, though its tooth thickness is not yet optimized, is somewhat smaller than that of the spherical involute bevel pinion. This fact indicates that the induced stress in IPB gears is surely considerably lower than that of the conventional bevel gears used today. There must exist some additional rooms beyond the results of this simulation to increase reliability, to make the gear box smaller and its weight lighter by incorporating IPB gears. This is the additional advantage of IPB gears, besides the efficient productivity. The potential for improved IPB gears is high.

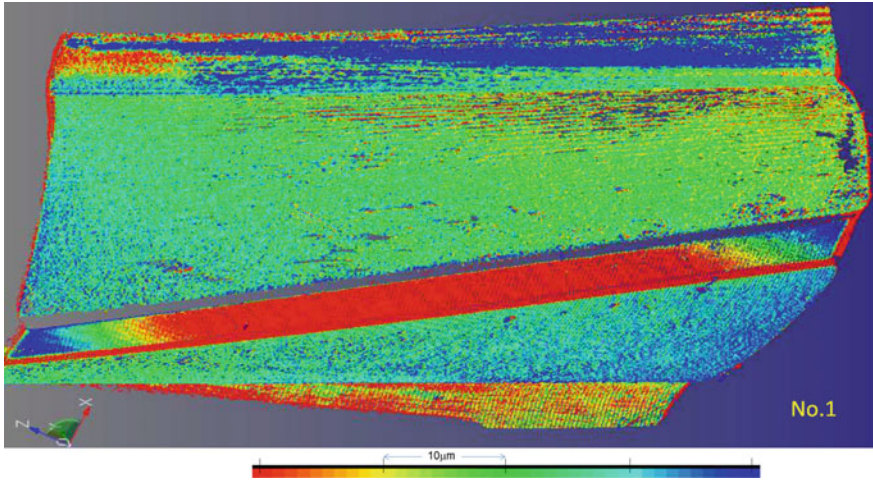


Fig. 11 3D tooth flank form deviation of an IPB pinion

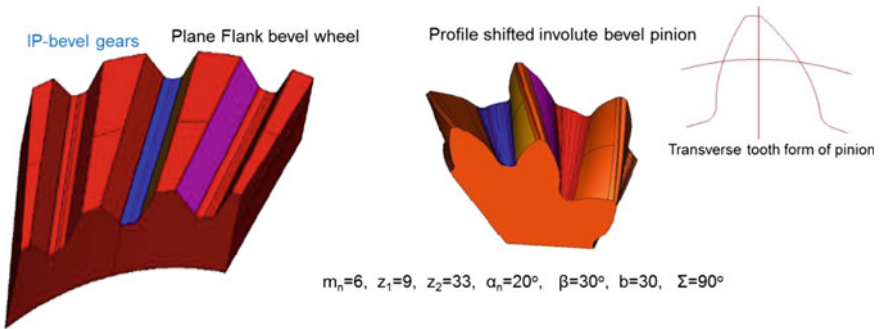


Fig. 12 Sample of IPB gears

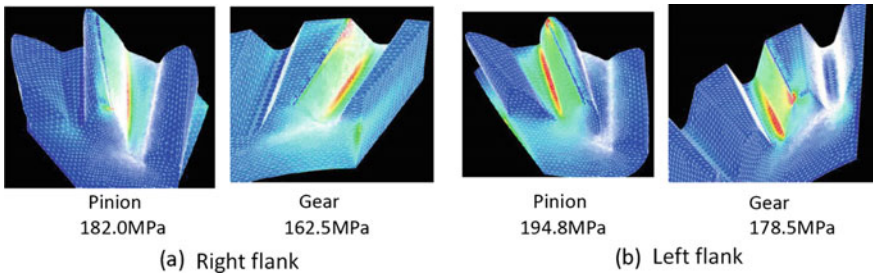
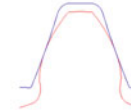
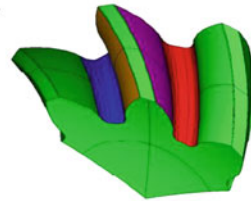
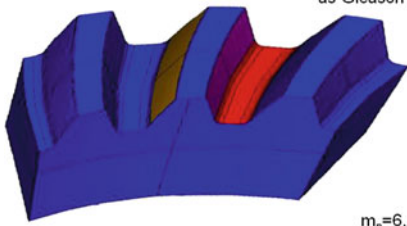


Fig. 13 Bending stress induced in an IPB gear

Spherical involute bevel gears

Tooth flank of pinion and wheel is spherical involute, tooth fillet is spherical trochoid. Tooth height and tooth width are selected as same as Gleason's gears.



Transverse tooth form

$$m_n=6, z_1=9, z_2=33, \alpha_n=20^\circ, \beta=30^\circ, b=31.1, \Sigma=90^\circ$$

Fig. 14 Sample of *spherical* involute bevel gears

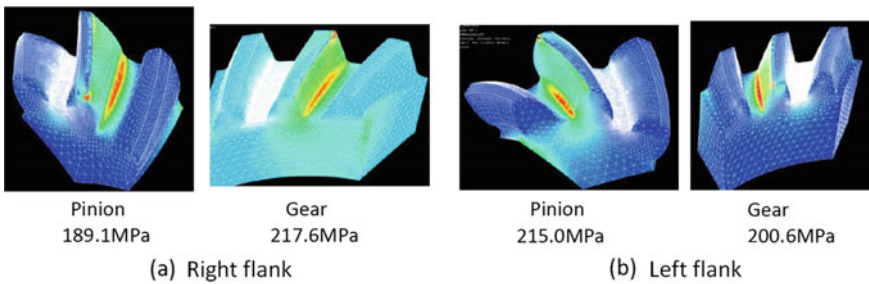


Fig. 15 Bending stress induced on *spherical* involute bevel gears

6 Surface Integrity of the Tooth Flank

Induced Hertzian stress as the index for surface durability is a function of the relative radii of contacting surfaces. The relative radii of the tooth flanks of IPB gears are somewhat larger than those of conventional bevel gears. We are therefore not anxious about the calculated magnitude of the contact stress. The problem could be the surface roughness of the finished tooth flank of IPB gears, when we deal with the surface durability of those same gears. Figure 16 shows the typical look of a tooth flank of an IPB wheel finished by one path of cutting with a $\phi 8$ mm flat end mill.

The horizontal stripes in the lead direction come from the different cutting capability of the milling tool blades in its axial direction. The magnitude between these stripes in the tooth form direction is not large, about $0.7 \mu\text{m}$, as shown in Fig. 17. The rippling figure of surface micro-geometry in the tooth lead direction comes from the eccentricity of the milling tool on the 5-axis machine. The magnitude of that ripple is about $0.8 \mu\text{m}$, but the mounting eccentricity of the milling tool must be considerably larger than this value. Such an amount of tool mounting eccentricity cannot be avoided. Figure 18 shows the enlarged figure of

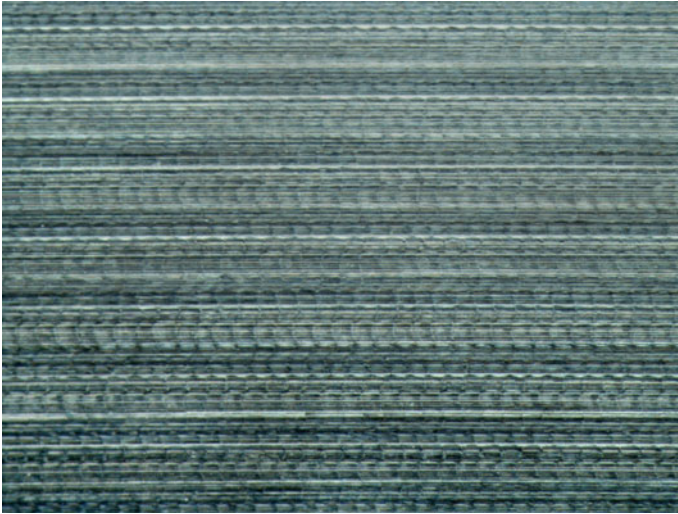


Fig. 16 Typical plane tooth flank of an IPB wheel finished by one path of cutting with a $\varnothing 8$ mm flat end mill

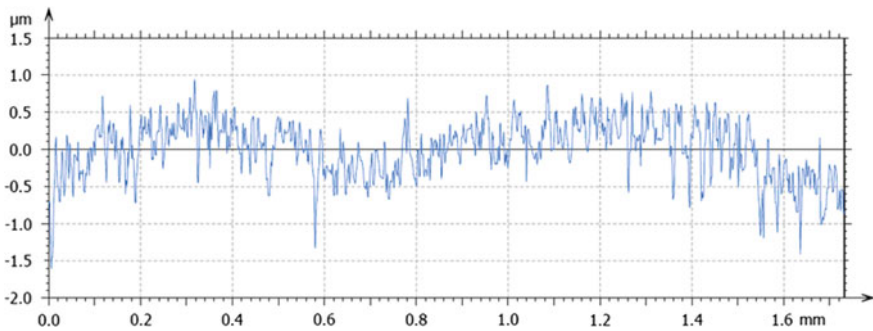


Fig. 17 Surface form of an IPB wheel tooth flank in the tooth form cross-section (figure sampled by $1\ \mu\text{m}$ pitch, with no filtering)

that surface. It is very interesting to find that cutting induces a small amount of very local melting of the cut surface. In certain places in the picture, you can see small black balls: those are the result of the melting of very local surface material by cutting. Melted material congeals. The diameter of the congealed steel ball is ca. $10\text{--}40\ \mu\text{m}$.

Figure 19 shows the tooth flank of an IPB wheel ground by one path of a CBN disk tool. Perhaps we have chosen too fine a CBN grain size of #400–500 for the grinding tool. The ground surface is almost mirror-like, but many very thin scratching traces can be observed, along with some regional, loose, mirror-like glare. We observe the surface as reflecting many colors, due to the diffraction of

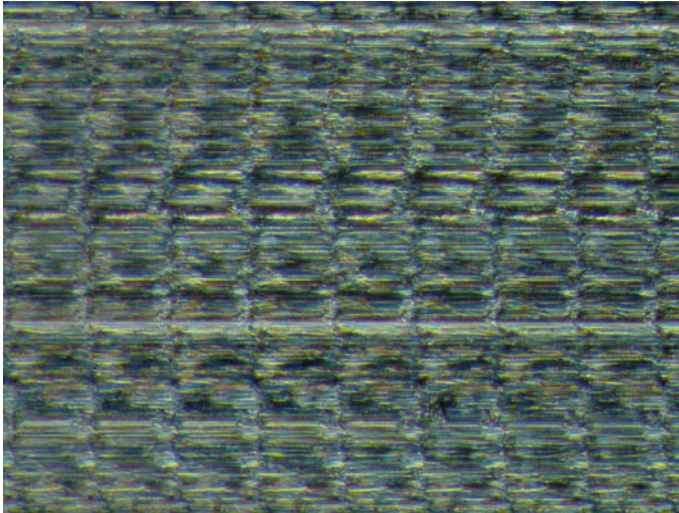


Fig. 18 Rippling due to eccentricity of tool, and small black balls as the evidence of local tooth flank melting at cutting



Fig. 19 Plane tooth flank of an IPB wheel finished by one path with a CBN disk tool

light. Figure 20 is the enlarged figure of the surface. It looks as if CBN grains have caused some deep scratching on the ground surface. Figure 21 shows a greatly enlarged picture of the surface, where the lighting is adjusted into a very soft, i.e., into a strongly scattered, light state. Thus, it is confirmed that the CBN grains have caused quite a number of groups of very shallow scratched grooves, the magic of light causing people to get the impression of deep grooves or ridges. The measured surface roughness is indicated in Table 1, and it is very fine. The grinding surface of the CBN tool cannot be set in a perfect, flat contacting state against the objective surface to be ground: the grinding surface of the tool can vibrate in sub-micrometer amplitude at grinding. The resulting ground surface features a stripe-like grouping

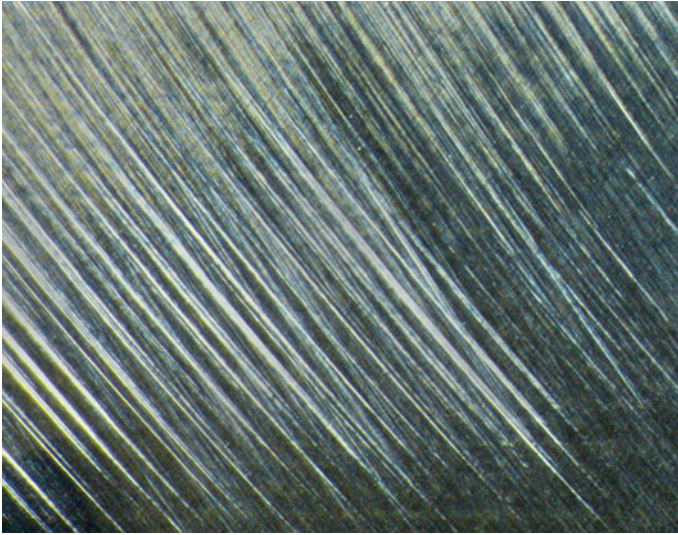


Fig. 20 Nominal ridges on the wheel flank

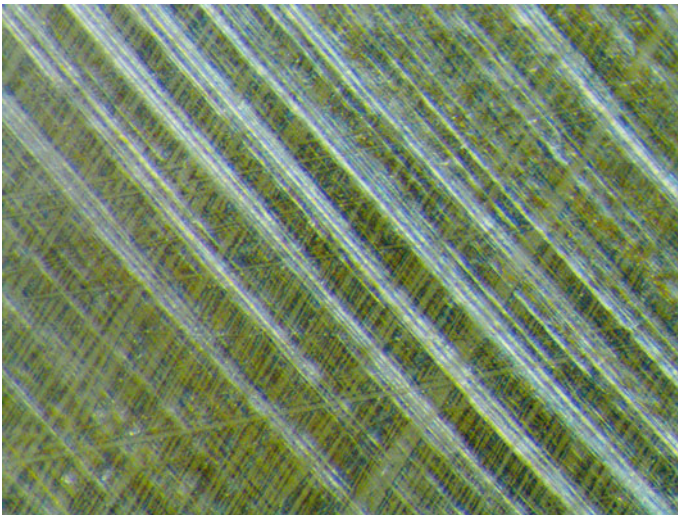


Fig. 21 Shallow groups of scratching on the wheel flank

of ground traces, i.e., like micro scratching, and the resulting distance between these stripes is almost equal.

Figure 22 shows an example of a detailed 3D figure of the tooth flank of the IPB wheel in Fig. 19. CBN grains have ground against the objective flank, causing fine grooves of 0.3–0.4 μm in depth. By the side of those grooves, slightly projected

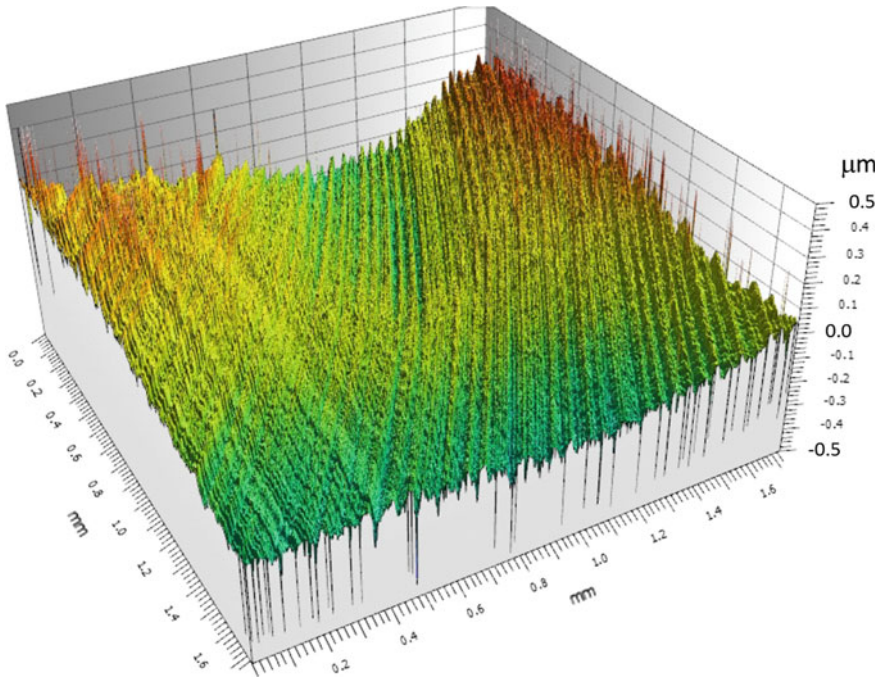


Fig. 22 3D figure of the ground flank of an IPB wheel (distance figure from the optical flat, sampled by 1 μm pitch mesh, with no filtering)

banks of plastically deformed surface material of less than 0.05 μm in height are generated.² Aside or on those banks, many small, ball-like objects of 0.1–0.3 μm in diameter adhere. Perhaps very local tooth flank material became plastically deformed and melted during grinding of the grain scratches into the objective tooth flank, and the melted surface material then congealed to become small ball-like objects adhering to the flank. In Fig. 22, they are expressed as a group of needles that exists by the side of the scratching grooves made with the grinding grains. This needle form, however, is the result of the big magnification difference in the z-direction, in comparison with the x- and y-directions in the figure configuration. The part of the tooth flank with the majority of such adhering chips or ball-like objects allows the glare outlook of the surface to look frosted.

Due to repeated contact of the grinding tool surface against the objective surface to be ground, or to a different state of lubrication between the grinding surface of the CBN grinder and the objective tooth flank, or to a slight imperfection in the tool mounting, or to tool vibration, the grinding disk makes contact with some parts of the tooth flank multiple times. That part of the objective tooth flank surface is ground slightly deeper, by 0.3 μm .

²The resolution of the measuring apparatus is 0.1 nm.



Fig. 23 Tooth flank of an IPB pinion finished by many paths with a CBN disk tool

Figure 23 shows the tooth flank of an IPB pinion finished by many paths of grinding with a CBN disk tool. The nominal grinding depth is $5\ \mu\text{m}$ and the step pitch of the tool path in the direction of the tooth form is $0.4\ \text{mm}$. Under such a grinding condition, the CBN grinding tool disk is not rigid enough, which means that the micrometer-order deformation of the tool disk is very easy. As a result, the stripe mark in the tooth lead direction due to tool feeding takes on a very obscure form. From the state of the scratching traces on the tooth flank, it is recognized that a considerably wide part of the disk flat of the grinding tool is making contact with the objective tooth flank of the pinion.

Tables 1 and 2 sum up the results of the residual stress of the surface material of the tooth flank and surface roughness to determine the nature of the finished tooth flank of IPB gears manufactured with a 5-axis machine. The residual stress, or to be exact, the residual lattice strain of the ferrite crystal of the tooth flank material, is investigated by using X-ray diffraction. The amount of compressive/tensile residual deformation and shearing deformation of the ferrite lattice is modified so as to obtain the stress dimension by multiplying the nominal elastic modulus. The full width at half maximum (FWHM) of the diffracted X-ray beam corresponds well to the Vickers hardness value at a depth of ca. $7\ \mu\text{m}$ from the surface. In the case of this material, 100 times the FWHM-degree value corresponds well to the micro-Vickers hardness, e.g., 6.03° . FWHM corresponds to ca. 600Hv.

The tooth flank ground by the CBN disk grinder is covered with traces of micro scratching due to the grinding grain movement and results in very smooth surface roughness. The surface hardness, however, looks to turn out a little lower than that of the milled tooth flank. It suggests the surface temperature at grinding with a CBN disk has the tendency to increase. The grinding tool, perhaps, rubs the target surface strongly. The residual compressive stress has some orientation concerning the direction of the grinding grain movement. Those results come from the fact that we

Table 1 Residual stress or ferrite crystal lattice deformation

		Cutting direction			Normal direction to cutting		
		σ_x (MPa)	T_{xy} (MPa)	FWHM	σ_x (MPa)	T_{xy} (MPa)	FWHM
CBN disc grain size #400–500	Wheel	-978	-93	6.03	-711	50	5.84
	Pinion	-901	128	5.89	-1044	-87	5.81
∅8 mm flat end mill	Wheel	-791	-148	6.38	-696	175	6.27
	Pinion	-548	-76	6.55	-731	192	6.24

Table 2 3D and 2D surface roughness

		Sz	Sa	Rz	Ra
CBN disc grain size #400–500	Wheel	1.7	0.06	0.46, 0.38	0.06, 0.04
	Pinion	2.76	0.07	0.56, 0.18	0.05, 0.03
∅8 mm flat end mill	Wheel	5	0.32	1.91, 0.88	0.21, 0.14
	Pinion	4.64	0.28	2.3, 1.31	0.36, 0.24
				Values max to min	

have chosen too fine a CBN grain size for the grinding tool. When we use grains of a somewhat rougher size, then the surface roughness becomes a little bit more pronounced, but deterioration of the ground surface concerning residual stress and hardness must be improved.

The milled tooth flank looks very rough, at least according to the impression given by such photos as those shown in Figs. 16 and 18, but the measured roughness value is not nearly as bad as one might suppose from the look of the photos. A 5-axis machine can produce gears comparable to those made with a hobber, a shaper, etc., for machining involute gears.

7 Bevel Gears to Come

Our development work shows that the performance of IPB gears can surely be a little bit better than that of conventional bevel gears. The number of tool paths needed to generate the tooth flank form of an IPB wheel decreases by more than 10 times that needed for conventional bevel wheel production, when a 5-axis machine produces it. We can surely produce an IPB wheel far more efficiently than a conventional bevel wheel. However, the problem remains for the production of an IPB pinion. When we produce an IPB pinion with a 5-axis machine, we need the same working time as for the production of a conventional bevel pinion. The basic tooth flank form of an IPB pinion is that of a conical involute gear with 3D micro-geometry correction. The amount of this tooth flank correction is usually less than 130 μm. One other problem will be the interference of the back side of the



Fig. 24 IPB gears in good mesh and smooth working

grinding wheel against the back flank of the pinion to be ground. That problem can be solved by the design of a proper grinding disk tool. It must therefore be possible to grind the tooth flank of a conical involute gear with a 3D flank form correction with today's better gear grinders, if a clever disk tool design is created and adequate numerical control software is supplied. Then, the production rate of the IPB pinion is improved to the level of cylindrical involute gears. The total production rate of IPB gears then becomes far better than that of the conventional bevel gear. Of course, there already exists a great amount of production machinery and facilities for conventional bevel gear production today, and it would cost too much to discard them to incorporate IPB gears. Perhaps in the field of bevel gear usage in which the amount of such already existing production facilities, and their accompanying inheritance, is comparatively small, IPB gears will be gradually incorporated (Fig. 24).

Acknowledgements The intention of this publication is that the technology concerning IPB gears should not be patented, for the benefit of the public throughout the world. The authors appreciate the agreement of the JSME RC268 committee members on this matter. The IPB gear is free to be used!